Mine Water Environ (2018) 37:56–74
DOI 10.1007/s10230-017-0470-4

TECHNICAL ARTICLE

Prediction of Acid Mine Drainage (AMD) and Metal Release Sources at the Küre Copper Mine Site, Kastamonu, NW Turkey

Nurgul Balci[1] · Cansu Demirel[1]

Received: 28 May 2016 / Accepted: 5 June 2017 / Published online: 15 June 2017

Abstract Waste and lithological rocks were subjected to aqueous leaching, acid base accounting (ABA), and net acid generation (NAG) tests, and detailed mineralogical investigations were conducted to predict acid mine drainage (AMD) formation at Turkey's largest historical copper deposits. The field water chemistry from springs and seeps on the mine site were compared with the static and long term aqueous leaching test results. During the ABA, NAG and long term paste pH tests, ore rich and ore bearing wastes showed a paste pH <4, implying their acid generating nature. The relationship between net neutralization potential and acid producing potential revealed that waste rocks with a low sulfur content were generally low potential sources of AMD. Consistent with the static test results, aqueous leaching tests revealed that greater concentrations of Fe, Cu, Zn, Ni, Pb, Cd, Co and As were released from the wastes rich in pyrite. The test methods all generally agreed that the ore-rich wastes (O, P1C, P1D) were the main sources of AMD and metal contamination in the district.

Keywords ABA static tests · Acid production · Aqueous leaching · Küre VMS copper deposits · Paste pH · Long term paste pH

Introduction

Acid mine drainage (AMD) is still a worldwide environmental problem despite extensive research on predictive and preventive techniques (Bouzahzah et al. 2013). When exposed to air and water, sulfidic wastes undergo atmospheric and aqueous oxidation and tend to generate acidic waters that often contain elevated concentration of sulfate, iron, and potentially toxic metals (Balci et al. 2007, 2012; Çelik-Balci 2010; Lottermoser 2010; Nordstrom et al. 2000; Sahoo et al. 2014; Schippers 2004). Acidic waters that originate from pyritic waste or ore can also be anomalously rich in trace elements such as Ni, Co, As, and Sb (Balci et al. 2012; Lapakko 2002).

Extended generation of AMD typically occurs when the rates of acid production exceed the neutralization capacities of the host rocks. Therefore, assessment of AMD generation involves both prediction of the acid production potential (APP) of waste materials and neutralization potential (NP) of lithological units located in the same environment. Various parameters and test methods are used to assess these factors. The most commonly used methods are static and kinetic tests (Brodie et al. 1991; Duncan and Bruyensteyn 1979; Hageman et al. 2015; Lapakko 2002; Lawrence et al. 1989; Lawrence and Scheske 1997; Modabberi et al. 2013; Plumlee 1999; Sobek et al. 1978). Static tests, also known as acid-base accounting (ABA) tests, were originally developed to predict AMD generation at coal mining sites and then modified for metal mines (Kwong 1993; Jambor 2003; Jambor et al. 2007; Sobek et al. 1978). ABA

Electronic supplementary material The online version of this article (doi:10.1007/s10230-017-0470-4) contains supplementary material, which is available to authorized users.

✉ Nurgul Balci
ncelik@itu.edu.tr

Cansu Demirel
cns_demirel@hotmail.com

[1] Department of Geological Engineering, Faculty of Mines, Istanbul Technical University, Maslak, 34469 Istanbul, Turkey

tests consist of an analytical procedure that allows one to calculate the acid production (AP) and NP of a material. They are inexpensive, simple, and efficient, but do not provide any information about weathering rates (Akabzaa et al. 2007; Jambor 2003; Modabberi et al. 2013; Perry 1998; Skousen et al. 2002; Sobek et al. 1978).

In a recent study, Bouzahzah et al. (2014) used static tests to assess the role of sample mineralogy in AMD predictive studies and emphasized the limitations of static tests. For example, it is not possible to predict long term acid generation potential and the weathering rate of a given sample using static tests. As a result, net acid generation (NAG), paste pH, and aqueous leaching tests are used in combination with static tests to accurately predict potential mine drainage. In this context, the aim of the current study was to predict AMD generation in the Küre volcanic massive sulfide (VMS) mining district using different static methods and to compare and evaluate the reliability of the various methods. The results of ABA, long term paste pH, paste pH, and NAG tests performed on the same samples were compared with the results of a long term aqueous leaching test, conducted to simulate long term weathering reactions, and field water quality data to predict the post-mining water quality and future metal release.

Description of the Study Area

The Küre VMS area, located in the Kastamonu province of the western Black Sea region of Turkey, is the largest and most productive copper district of Turkey (Fig. 1). The Küre deposits were mined by the Genoese, Byzantines, and the Ottoman Empire (400–1000 years ago) and relicts of the ancient mining, such as old slag dumps, are still located north of Küre (Bailey et al. 1966; Güner 1980). Despite its long mining history, no data existed that could be used to predict the area's AMD potential. Exploitation of the recently discovered Mağarodoruk deposit, with a 2.15% Cu grade and 23,500,000 tonnes (t) of reserve, and located near the Küre Mountains National Park, underline the need for accurate AMD predictive studies (Akbulut et al. 2016; Altun et al. 2015).

Precipitation in the mine area is lowest in July and peaks in May; the area's annual rainfall averages 696 mm. July is the hottest month of the year, averaging 18.3 °C, and January is the coldest month, averaging below 0 °C. The average temperature year-round is 9.2 °C. The mining district is about 1500 m above sea level.

The Küre VMS deposits is mostly covered by the Küre Complex, which is also referred to as the Küre ophiolites (Okay et al. 2006, 2015; Fig. 1). Below the ophiolites are ultramafic rocks, comprising serpentinized peridotites and serpentinites tectonically overlain by massive and pillow lavas, with lava breccias at the top (Boztuğ et al. 1995; Çakır 1995; Ustaömer and Robertson 1994). Deep-sea sediments known as the Akgöl formation depositionally cover the Küre ophiolites, which consist of folded and well bedded gray-dark gray sandstones or graywackes and highly deformed black shales, with locally interbedded limestones (Bailey et al. 1966; Boztuğ et al. 1995; Güner 1980; Ustaömer and Robertson 1994). The Cyprus-type Küre VMS ores are located along the contact zones of the black shales and pillow lavas of the Küre Complex and were deposited via mineral rich hydrothermal fluids travelling through fault cracks (Çakır 1995; Kuşçu and Erler 2002).

The Küre deposits are variously massive lenses, stock works, or disseminated in the host rock, with decreasing ore grade, respectively, and are mainly composed of pyrite and chalcopyrite (Akbulut et al. 2016; Altun et al. 2015; Bailey et al. 1966; Güner 1980). The main gangue minerals are quartz, calcite, dolomite, and chlorite (Akbulut et al. 2016; Altun et al. 2015).

Materials and Methods

The sampling points were selected based on the lithology and mineralogy of the mining district (Fig. 1). The waste rocks were divided into two groups: 1-unoxidized, fresh ore-rich rocks (O, n = 6) collected from the active underground mine site to predict maximum acid production rate for the district and 2-waste materials deposited on the surface (OBR1, OBR-2, OBR-3, P1C, P1D, P10A, and P10B). In addition, samples were collected from the gossan outcrop (n = 6, Gossan) of the Bakibaba open pit mine area, flotation tailings (n = 3; WEP) and s from various lithological units such as basalt (B, R2, R4, R5, P1A, and P1B), greywacke (R1 and R10), black shale (P1E and R3), limestone (R9 and P10C), and sandstone (i51, i52) for the current study (see Table 1). Each sample location recorded by GPS (in UTM coordinates) was plotted on the geological map of the area (Fig. 1).

Water samples were also collected during the field campaign. Acidic (n = 2; GW1, GW3) and neutral groundwater (n = 3; GW2, GW4, GW5) were sampled from the adit walls of Bakibaba underground mining tunnels at different elevations. Representative AMD surface water (n = 3; AMD1-3) and pristine neutral surface water (n = 2; SW) were also collected from the Karanlık Stream and Küçükali Stream, respectively (Fig. 1). Physicochemical parameters (pH, EC and Eh) of all the water samples were determined in situ using a WTW-330 probe. In addition, an extra 50 ml water sample from each sampling point was filtered (0.2 µm Sartorius syringe filter) and acidified with research-grade 1/10 diluted HNO_3 to further analyze metal contents. The sulfate content of each water sample was determined in-situ

by Hach-2800 spectrophotometry. The metal concentrations of water samples were analyzed by inductively coupled plasma mass spectrometry (ICP-MS; PerkinElmer Analyst 300) at the ITU Material Sciences and Production Technologies Applied Research Center.

The mineralogical compositions of the powdered rock and waste samples were detected using Bruker D8 advance X-ray diffraction (XRD) between 2 and 70° theta angles with a Cu target. Side-loading aluminum holders were used for XRD studies. Polished thin sections were prepared from the ore bearing waste rocks (OBR-1, OBR-2, OBR-3) and investigated using a Nikon LV100 ore microscope. The bulk chemical composition of the samples (Fe, Mg, Ca, K, Al, Na, Mn, Cu, Zn, Ni, Co, Ti, Pb, Cd, As) were determined by inductively coupled plasma-atomic emission spectrometry (ICP-AES) following acid digestion with a HCI-HNO_3-$HCIO_4$-HF mixture. The silica content was determined by ICP-AES following Na_2O_2/NaOH fusion. An X-ray fluorescence spectrometer (XRF; Philips PW2400) was used to determine the total S content of each sample following $LiBO_2$ fusion.

AMD Prediction Static Tests

The following methods were used to determine the AP and NP of the samples: acid production potential (APP), net neutralization potential (NNP), neutralizing potential ratio (NPR), maximum potential acidity (MPA), net acid

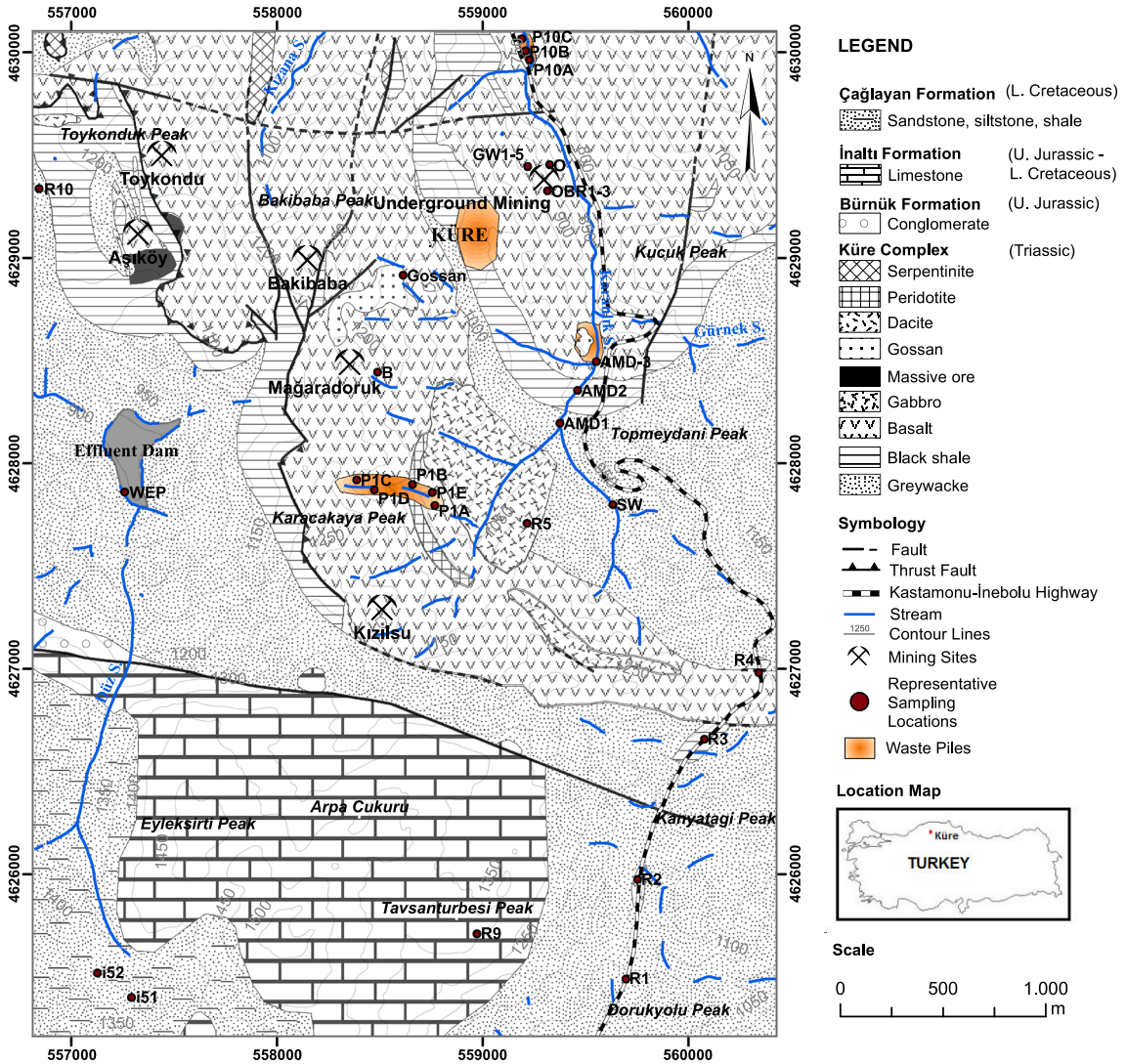

Fig. 1 Geological map (in UTM coordinates) showing stratigraphic units and sampling locations around Küre VMS deposits, modified from Bailey et al. (1966); Güner (1980) and Okay et al. (2014, 2015)

generating pH (NAG_{pH}), and NAG tests, in addition to acid neutralization capacity (ANC) and net acid-producing potential (NAPP). The APP, NNP, NPR, NP, MPA, ANC, NAPP, and NAG value of each sample was calculated (Supplemental Tables 1 and 2). All of the rock samples were dried, grinded, and sieved to the various particle sizes required for the different methods. In the ABA study, the paste pH and paste EC of each sample were determined using a pH/EC meter (WTW-330 probe).

The NP was calculated following the methods proposed by Sobek et al. (1978). The first step in determination of NP involves a fizz test, which is used to estimate the calcium and magnesium content of a sample. The fizz test was performed by reacting the sample with diluted hydrochloric acid at room temperature (Supplemental Table 2). Following the determination of the fizz rating test, the specified amount of HCl with given normality was added to the sample and placed into pre-heated water bath at 85 °C until the reactions were completed. Then the mixture was cooled and back titrated to pH 7.0 with NaOH of the same normality. The amount of NaOH added was then used to determine how much HCI was neutralized by the sample. The NP value of each sample was calculated according to the formula given in Supplemental Table 1 and reported as kg of $CaCO_3$/t of rock.

The NAG test was used along with ABA to classify the APP of the samples. The NAG test is based on the reaction of a sample with hydrogen peroxide acting as quick oxidizing agent for sulfide minerals present in a sample. Since acid generating and neutralizing reactions co-occurs in a sample, a final result of NAG test directly represent of the net amount of acidity produced by the sample and is calculated as kg H_2SO_4 per ton of the material. For the NAG test, 15% hydrogen peroxide heat-extraction and NaOH titrations were performed (Miller et al. 1997). Each sample was rapidly oxidized and the NAG_{pH} values were recorded. The NAG of each sample was determined based on the volume and concentration of base used in the tests (Supplemental Tables 1 and 2), as in previous studies (Lottermoser 2010; Miller et al. 1997).

Paste pH experiments were performed for each sample using ultrapure water as the only reagent with 100% pulp density (Page et al. 1982; Sobek et al. 1978). Physical parameters (Eh, pH, and EC) were frequently monitored for three weeks. After each measurement, the mixtures were stirred with a glass stick and the beakers were resealed with Parafilm M bands.

Long Term Aqueous Leaching test

The leaching test was performed under conditions analogous to the natural environment (e.g. with simulated rainwater). The leaching tests were performed on the same samples used for the static tests to predict long term acid generating potential and metal release capacity. The leaching test was applied to splits of the samples at the Istanbul Technical University (ITU) Geomicrobiology Laboratory for 3 months. The splits were combined with simulated rain water at a ratio of 20:1. The mixtures were shaken for 5 min and the experimental beakers were aerated daily by removing their parafilm cover for an hour and stirring the contents with a glass stick for 5 min. After 3 months, the leachates were filtered (0.2 µm Sartorius syringe-tip filter) and divided into two parts. One part was used to analysed for metals with the ICP-MS and the other portion was used for anions (SO_4^{2-}, NO_3^-, NH_4^+, CI^-, and F) and cations (Mg, Ca, K, Na) with ion chromatography (IC-Perkin Elmer). The pH and EC measurements were made at the end of each experiment. Based on the leaching test, the long-term paste pH test was proposed and used to predict acid generation and neutralization consumption along with the other ABA tests.

Results and Discussion

Bulk Geochemistry and Mineralogy of the Samples

Detailed mineralogical and chemical characterization of a sample is a crucial step in AMD prediction at mining sites. The concentrations of major, minor, and trace elements in all samples used in the static tests are presented (Table 1), along with their crustal abundance (CA) values (Wedepohl 1995).

The ore-rich and ore-bearing waste rocks display significant concentration of Fe, S, Cu, Zn, Co, Pb, and As. The highest concentration of Fe, 36.9 wt %, was found in the ore-bearing waste rocks (P1C, O), which was predominantly pyrite (Table 2). Between 7 and 31% of the waste rock mass was Fe. The rest of the samples belonged to various lithological units in the study area and contained 0.4–13.23% Fe, with a few samples (P1E, P1B, and R2) also containing significant Fe concentrations. Copper and zinc were the dominant other metals, with the highest concentration of 44,010 and 27,430 ppm in the ore-rich rock, respectively. In general, the ore-rich samples (OBR1-3; P1C, P1D, P10A, P10B) contained significant amounts of Cu and Zn (Table 1). Concentrations of Zn in all samples, and particularly in ore bearing and rich waste, were greater than the CA (65 ppm). The areas of limestone, shale basalts, and calcite (R9, R10, P10C, i51, i52; Table 2) were the only ones that did not exceed the CA value for Cu. The flotation tailing (WEP) and gossan contained elevated concentrations of Cu, Zn, and Fe in addition to Co, Pb, and Cd. The Co, Pb, Cd and As concentrations in the ore-rich (O) and ore-bearing waste rocks (OBR1-3, P1C, P1D, P10A,

Table 1 Major oxides and selected metal composition of the samples subjected to AMD prediction static tests

Sample	SiO_2 (%)	Fe_2O_3 (%)	Al_2O_3 (%)	MgO (%)	CaO (%)	Na_2O (%)	K_2O (%)	Fe (%)	Cu (ppm)	Zn (ppm)	Co (ppm)	Ni (ppm)	Ti (ppm)	Mn (ppm)	Cr (ppm)	Pb (ppm)	Cd (ppm)	As (ppm)
Waste rocks																		
O	0.07	50.96	0.16	0.66	0.51	0.51	0.09	35.64	44,010	27,430	1776	19	56	10	5	385	52	613
OBR-1	5.32	27.46	25.86	17.02	2.30	0.73	0.09	19.17	180	420	616	191	569	180	316	24	22	16
OBR-2	3.53	44.10	22.04	10.88	1.70	0.51	0.06	30.84	530	300	539	148	2215	320	305	15	16	6
OBR-3	1.14	36.49	15.13	9.72	2.27	0.71	0.10	25.52	70	390	226	118	2701	170	267	27	22	11
P1C	0.09	52.18	5.50	3.36	0.48	0.62	0.09	36.93	14,410	2670	1561	32	671	30	48	64	22	170
P1D	0.56	10.76	22.21	11.66	7.53	3.14	0.45	7.53	700	450	137	66	5120	1160	152	25	22	6
P10A	2.21	24.29	9.29	4.48	25.82	0.51	0.10	16.99	780	410	156	35	2390	630	95	29	18	14
P10B	0.18	9.94	0.74	0.77	0.64	0.59	0.11	6.96	170	320	34	26	1831	1200	119	32	16	33
Gossan	5.31	22.46	20.39	9.65	0.80	0.60	0.07	15.71	490	410	31	4	483	1	25	28	18	68
WEP	0.21	30.10	7.08	3.47	4.80	1.07	0.45	21.06	4230	4430	1287	37	1006	390	68	228	33	246
Lithological units																		
B	0.27	8.81	19.93	14.98	4.23	3.30	0.65	6.16	170	410	69	123	3080	1430	341	18	19	4
R1	10.34	2.58	14.31	1.87	5.72	2.71	1.43	1.81	20	280	29	24	1270	230	60	26	19	44
R2	8.54	13.31	12.21	9.29	5.49	1.47	0.20	9.31	120	240	101	107	2596	471	203	16	18	12
R3	2.41	9.43	22.41	4.11	6.66	1.41	2.37	6.6	140	410	38	109	2036	1300	101	52	24	60
R4	16.83	8.45	18.40	8.66	9.31	5.39	0.25	5.92	40	290	45	53	4812	960	144	17	18	48
R5	13.90	7.84	21.05	5.45	7.91	7.57	0.20	5.48	30	280	35	1	3855	720	18	20	21	10
R9	0.62	0.07	0.08	1.48	27.53	0.56	0.05	0.0005	20	300	10	18	807	90	33	21	17	7
R10	18.12	2.65	16.96	2.12	6.24	3.58	1.61	1.85	20	400	31	27	1370	200	130	32	21	19
P1A	9.97	6.37	22.31	14.83	6.74	5.80	0.97	4.46	90	430	40	91	1718	730	247	24	22	9
P1B	7.26	14.76	7.38	30.61	5.38	1.12	0.15	10.33	950	350	126	921	1522	1140	299	17	16	6
P1E	8.74	18.91	23.63	4.49	4.94	0.75	1.93	13.23	600	490	58	116	2087	24,380	158	80	20	25
P10C	0.46	0.48	0.02	1.04	44.87	0.50	0.08	0.34	20	250	7	2	1051	1530	20	19	15	5
i51	21.79	4.17	12.24	2.76	8.04	2.48	0.93	2.92	10	360	47	35	831	330	115	53	17	19
i52	8.10	0.55	10.60	0.99	3.04	2.32	1.41	0.39	10	370	16	4	880	20	54	163	16	9
CA								43,200	25	65	24	56	4010	716	126	14.8	0.1	1.7
AALC(ppb)									65	120		120				65	<2	

CA crustal abundance (Wedepohl 1995), *AALC* Acute Aquatic Life Criterion

P10B) were significantly higher, and the average Co, Pb, Cd, and As concentrations in the waste rocks (except for the gossan and WEP samples) exceeded CA values by 631 times, 75.1 times, 23.8 times, and 108.6, respectively.

The highest Co, Pb, Cd, and As concentrations were found in the ore-rich wastes (1776, 385, 52, and 613 ppm, respectively), though the flotation tailings also contained high Pb, Cd, and As concentrations. The lowest Ti, Mn, and Cr concentrations were found in the ore-rich samples (56, 10, and 5 ppm, respectively). The highest Cr concentration was in the basalt sample (B). In general, samples low in sulfur and ore minerals (such as pyrite) contained significant amounts of Ti, Mn, Cr, and Ni. The highest Cd concentrations were found in the ore-rich (O) and WEP sample (52 and 33 ppm, respectively). Total base metals (Cu + Cd + Co + Ni + Zn + Pb) generally increased with Fe content and decreased with an increase in major cations (Fig. 2a, b). The base metal and Fe content of the flotation samples (WEP) were comparable to the ore-rich waste rocks (OBR1-3, P1C; Fig. 2b). In general, samples with low Fe and base metal content belonged to lithological units with a high major oxide content and high neutralizing potential. The highest major oxide content belonged to P10C sample, which had the lowest base metal content. Except for OBR-1, P10A, and P1D, waste samples with high APP showed high base metal and low major oxide trends (Fig. 2). In the Küre VSM district, the samples with greater base metal and lower major oxide content were the waste rocks, gossan, and WEP. The waste samples rich in ore (O, OBR1-3, P1C, P10A, and P10B) generally consisted of pyrite, chalcopyrite, and minor amounts of sphalerite, and had high APP, with quartz and chloride as abundant gangue phases. In the OBR-2 and OBR-3 samples, chalcocite (Cu_2S) and covellite (CuS) were also present (Table 2). In general, the main gangue phases in all of the samples were quartz, chlorite, illite, muscovite, and feldspar. Gossan is composed of hematite and quartz. The WEP sample contained both of the ore minerals, mostly pyrite, and gangue phases of quartz and clay minerals in addition to secondary sulfates, such as gypsum and jarosite. Lithological units and waste rock samples with low sulfide content mainly contained quartz, albite, chlorite illite, muscovite, calcite, amphibole, talc, plagioclase, olivine, and serpentine, with some local vein-filling (R2) or disseminated pyrite (P10A, P10B). In general, chlorite was the most common sheet silicate, with lesser amounts of muscovite. Clay phases included kaolinite, talc, montmorillonite, and illite (Table 2).

Microscopic investigation of the waste rock samples (O, OBR-1, P1C, and OBR-3) showed paragenetic relationships between the pyrite, chalcopyrite, hematite, and magnetite (Fig. 3). Most of the pyrite grains in the ore bearing rocks had deformed anhedral morphology, along with some subhedral and locally euhedral cubic grains. These were either large grains containing chalcopyrite and specularite within or in their fractures; or as relatively small grains disseminated in the host basalt. Euhedral pyrite oxidizes slower than disseminated pyrite, which will oxidize quickly due to its larger surface area (Weber et al. 2004; Weisener and Weber 2010). Although elevated acid generation rates can be expected from disseminated reactive pyrite oxidation, acid generation can also be severe from large pyrite particles and euhedral pyrite (Schippers 2004). Waste samples rich in pyrite (O, P1C, and WEP) are generally acid generating, irrespective of the oxidizing agent (Fe(III) or O_2), but chalcopyrite oxidation is only acid generating when the oxidizing agent is Fe(III). Oxidation of pure sphalerite, covellite, and chalcocite are not acid-generating reactions (Balci et al. 2007, 2012; Plumlee 1999). This is consistent with the ABA static test results, in which samples O, P1C, and WEP, which were rich in pyrite, was acid producing, while OBR1, which contained minor amounts of pyrite, chalcopyrite, sphalerite, and a sulfur content of 1%, was not (Table 2).

Acid Generation and Neutralization Capacity of Wastes and Lithological Rocks

ABA static tests have been widely used to quantify the AP and NP of geologically diverse mine wastes (Bouzahzah et al. 2014; Sahoo et al. 2014). In addition, NAG along with the ABA tests have been applied to different wastes such as Pb–Zn tailings (Shu et al. 2001) and metallogenic belts (Akabzaa et al. 2007) to obtain more robust predictions. The combined results of paste pH, long-term paste pH, ABA, and NAG tests are presented in Table 3 and the test results were evaluated based on the various screening criteria developed over the years by various researches (Tables 4, 5).

Based on the paste pH results, most of the waste and lithological units can be classified as non-acid generating except for samples O, WEP, and PIC, since a paste pH <4 is considered as acid-toxic (Sobek et al. 1978; Table 4). The long-term paste pH tests, used for the first time in the current study, compared well with the paste pH tests and indicated the most samples were not acid generating (Table 3). The consistent results among the different paste pH tests suggest that common paste pH test is a convenient and reliable method to predict long term changes in pH of a waste exposed to rain. The long term paste pH results also showed that long term storage of waste materials, except for samples O, P1C, and WEP, produced slightly alkaline solutions.

The paste EC and long term paste EC values were also consistent. EC values ranged from 94 to 9650 µS/cm for the 3 week tests and from 112 to 9200 for the long-term

Table 2 Description and mineral content of the samples subjected to AMD prediction static tests

Sample	Description	Mineral Phases (XRD)
Metal and/or ore rich samples		
O	Pyritic copper ore (675 m)*	Pyrite, chalcopyrite, quartz, sphalerite
OBR-1	Disseminated ore in basalt (645 m)[a]	Chlorite, pyrite, chalcopyrite, quartz, sphalerite, magnetite
OBR-2	Disseminated ore in basalt (630 m)[a]	Chlorite, hematite, covellite, chalcopyrite, pyrite, chalcocite
OBR-3	Disseminated ore in basalt (512 m)[a]	Chlorite, covellite, chalcocite, pyrite, chalcopyrite, illite, quartz, sphalerite
WEP	Ore and waste bearing sludge (flotation tailings)	Pyrite, gypsum, quartz, montmorillonite, chlorite, jarosite, chalcopyrite, calcite, illite, dolomite
P1C	Pyrite rich waste	Pyrite, chlorite, chalcopyrite, quartz
P1D	Pillow lava	Disseminated ore, plagioclase, chlorite, quartz, talc, kaolinite, olivine, hornblende, calcite
P10A	Basalt with disseminated ore and calcite veins	Quartz, chlorite, calcite, forsterite, pyrite
P10B	Basalt with disseminated ore	Calcite, quartz, chlorite, pyrite
Gossan	Reddish-brown gossan outcrop	Quartz, hematite
Lithological units		
B	Basalt	Chlorite, albite, quartz
R1	Greywacke	Quartz, muscovite, feldspar, chlorite
R2	Basalt with pyrite vein	Chlorite, quartz, feldspar, pyrite
R3	Black shale with orange-red alteration surface	Quartz, chlorite, illite, feldspar, hematite
R4	Basalt	Feldspar, chlorite, illite, quartz, calcite
R5	Heavily alterated basalt	Feldspar, chlorite, quartz, calcite
R10	Greywacke-shale	Quartz, muscovite, feldspar, chlorite
P1A	Basalt	Quartz, feldspar, chlorite, amphibole, dolomite, calcite, gypsum, pyrite
P1B	Basalt-Basaltic andesite	Talc, chlorite, plagioclase, amphibole, hornblende, lizardite, olivine
P1E	Black shale	Quartz, chlorite, muscovite, calcite (magnesian), olivine
P10C	Quartz bearing milky-white calcite vein	Calcite, quartz
R9	Massive limestone	Calcite, quartz
i51	Medium-grained sandstone	Quartz, chlorite, feldspar, muscovite, calcite
i52	Medium-grained sandstone	Quartz, muscovite, feldspar

[a]Samples that were collected from different elevation level of Bakibaba mining tunnels, above sea level

tests (Table 3). Higher paste EC values with lower paste pH values in the O, P1C, and WEP samples indicated higher sulfide mineral oxidation rates and greater release of metals into the solution (Table 5). The waste samples (O, PIC, Gossan) and rock sample (R2) had low NP values, ranging from −217.5 to −6 and −5.0 kg $CaCO_3$/t, respectively (Fig. 4). The ANC of the respected samples correlated perfectly with the NP values (−213.15, −6.37, −5.88 and −4.9 kg H_2SO_4/t) of ore, respectively. The lowest NP value was associated with the waste samples (O) that contained an abundance of massive pyrite and chalcopyrite (Figs. 4, 5). The rest of the samples had NP values ranging from 2 to 792. 5 kg $CaCO_3$/t, consistent with the ANC values. The highest NP and ANC values belonged to the P1E sample (containing calcite, chlorite, quartz; Fig. 2a). The APP and MPA values varied widely, from 0.3 to 591 and from 0.6 to 578.3 kg of H_2SO_4/t, respectively. The APP and MPA values indicated that the maximum AP in the region was obtained from the O samples (591 ppt and 578.34 kg H_2SO_4/t), with a net acidity of about 206 kg H_2SO_4 per ton of ore (Table 3; Figs. 4, 5), respectively. The APP and MPA results correlated well and showed that the higher values were associated with the amount of pyrite and chalcopyrite in the sample (Fig. 5). The calculated NNP ranged between −808.5 and 686.5 kg $CaCO_3$/t in the waste samples and between −14 and 785.8 kg $CaCO_3$/t in the rocks. The NAPP values were consistent with the NNP.

The NAG test was used to verify the ABA tests and to determine the APP of the samples. In contrast to ABA, the acid generation reaction from pyrite oxidation and neutralization from the rest of sample can co-occur, with the final acidity directly measured in the NAG test. Therefore, overestimated acid production, which can occur when the total sulfur concentration is used (assuming that all of the

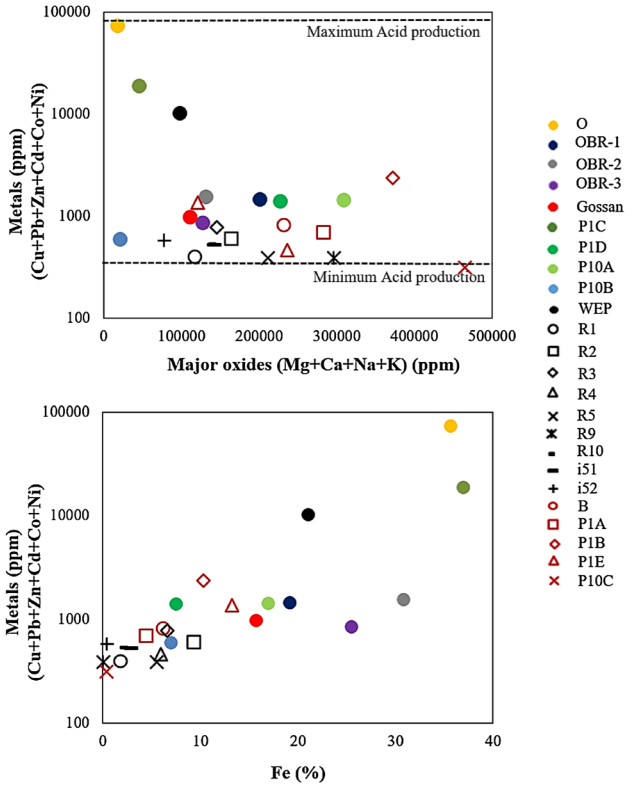

Fig. 2 Total base-metal concentrations versus major cations (**a**) and Fe content for the samples (**b**)

sulfur is pyritic) should not occur with this method. Sample OBR-3 was not subjected to the test due to its neutral initial leachate characteristic. NAG values are presented in Table 3 and ranged from 0.35 to 206.5 kg H_2SO_4 t^{-1}; the NAG pH ranged between 2.39 and 7.51. From the relationship between NAG and NAG_{pH}, O, OBR-1, WEP, and P1C can be considered highly acid generating, while R2, R3, i52, and P10A can be grouped as moderately acid generating, and the rest grouped as non-acid generating (Fig. 6; Sahoo et al. 2014). Despite its uncertain character in ABA tests and its high paste pH, OBR-1 showed a high NAG value of 100 kg H_2SO_4 t^{-1} and a low NAGpH of 2.5. The OBR-1 sample contained sphalerite as the ore mineral with a sulfur content of 1.1% and it is likely that the sphalerite reacted with the peroxide, and produced acid, in contrast to its slow reaction rate in the ABA tests. This determination emphasizes that mineralogy affects predictive accuracy of APP and NP and suggests that the ABA and NAG tests results should be considered together for an accurate environmental assessment.

Although there is no common consensus, various ABA classifications are used to assess non-acid, uncertain, and acidic materials, based on paste pH, NNP, and NPR (NP/AP ratio) in addition to NAG and NAGpH (Tables 4, 5). Table 5 presents the consistency of the various methods. According to the NPR^1 (NP/APP) criteria, most of the samples (70%) were not acid generating with a NPR value >4, OBR-1 was possibly acid generating, O, P1C, WEP, R2, P1A, P1D, and Gossan were acid generating, with a NPR value <1 (Price et al. 1997). From the NPR^2 and NPR^3 criteria, it is clear that the O, WEP, R2, Gossan, P1A, P1C, and P1D samples had the potential to generate acid, with a NPR value of <1 (Fig. 4; Soregaroli and Lawrence 1998; Brodie et al. 1991). The OBR-1 sample was inconclusive according to all of the NPR criteria.

The waste samples O, WEP, and P1C can clearly be grouped as acid generating based on all three NNP^4, NNP^5, and NNP^6 criteria whereas Gossan, R2, and P1A grouped as acid generating based on the NNP^5 and NNP^6 criteria and uncertain according to the NNP^4 (Fig. 5). The rest were alkali generating, though a few of them cannot be strictly classified into either group (NNP^4 ranged between −20 and 20 ppt). The paste pH, long term paste pH, and ABA test results were quite consistent, suggesting that the paste pH test method can provide significant information about the leaching characteristics of materials.

Based on the various criteria and calculations, all of the tests agreed that O, WEP, and P1C were acid producing. Gossan and R2 were acid forming in $NPR^{1,2,3}$, $NNP^{5,6}$, and NAG^7 but NPR^4 and NAG^8 were uncertain; note that the superscript numbers in this paragraph all refer to Table 5. Sample R2 with its basalt and pyrite mineralogy, classified as acid generating, highlighting the importance of sulfide mineral content and points to potential local AMD generation. In contrast, despite its near neutral paste pH 7.6 and its low sulfur content (0.3%), the Gossan sample exhibited a very low NP (−6) and is considered acid generating. This result may indicate that a high percentage of iron oxides along with nearly no carbonate mineral content can be considered a limiting factor for the ABA test. P1D was considered as acid forming in the NPR method and in all NPR criteria and in the NNP method with the NNP^6 criteria, uncertain using the NNP^4 criteria and NAG^8 test, and non-acid forming according to NNP^5 and NAG^7. P1A was classified as acid generating in NPR, uncertain in the NNP^4 method and NAG^8 test, and non-acid forming in NAG^7. P10A was non-acid forming in all test methods except in the NAG^7 test. The rest of the samples were considered as non-acid forming in all methods except for sample R3, which was uncertain in NAG^7 (Fig. 6). Although our results suggest that there was a consensus in all methods, the NAG test with criterion 8 and NNP with criterion 4 were unable to accurately predict the character of the sample. In general, the silicates, common in all the samples, are known to contribute minimally to acid neutralization due to their slow dissolution kinetics. Therefore, some samples (P1D, R2, P1A, and i52) were uncertain according to the NNP method with criterion 4.

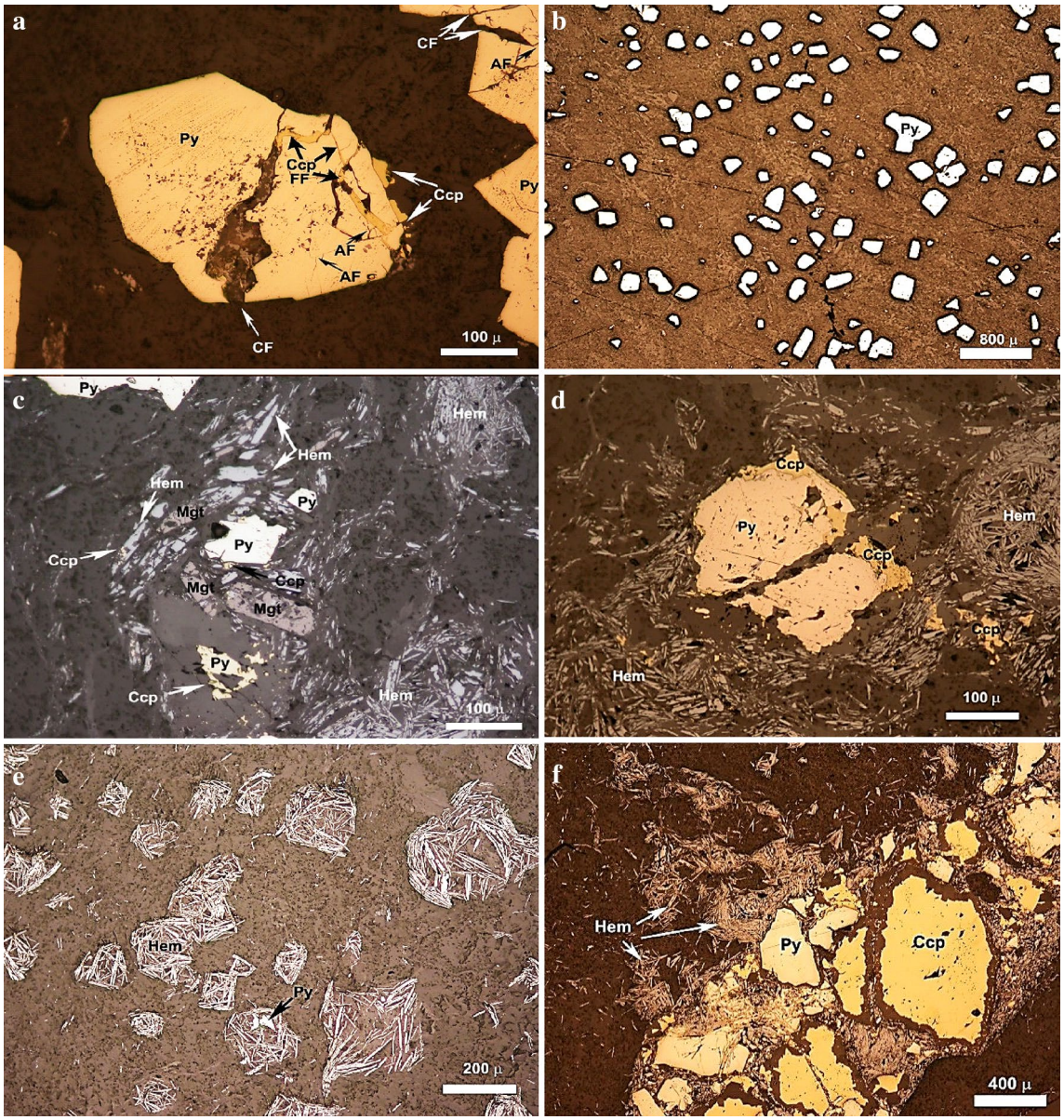

Fig. 3 Microscopic imaging of OBR's (*Ccp* chalcopyrite, *Hem* hematite, *Mgt* magnetite, *Py* pyrite, *AF* annealing fracture, *CF* cataclastic fracture, *FF* fracture filling). **a** Pyrite grains having chalcopyrite fracture fillings, cataclastic and annealing fractures in OBR-1. **b** Disseminated pyrite grains in the matrix in OBR-1. **c** Pyrite grain being substituted by chalcopyrite and surrounded by specularite in OBR-2. **d** Pyrite, chalcopyrite, specularite and prismatic magnetite in OBR-2. **e** Specularite clusters in OBR-2. **f** Paragenetic relationship between pyrite, chalcopyrite, and specularite in OBR-3

With reference to Tables 3, 4 and 5, all parameters calculated for different methods, including APP, NP, NNP, ANC, MPA, NAG, and NAGpH, are in good agreement with respect to AMD generation, as demonstrated in previous studies (Brady et al. 1994; Mohammadi et al. 2015; Sahoo et al. 2014). In general, these studies identified the importance of NP, NNP, and the NP/MPA ratio for predicting post-mining water quality. Skousen et al. (2002) further demonstrated that NP/MPA ratios were a better predictive criterion and suggested that NP/MPA ratios <1 should produce acidic effluent while ratios >2 should produce net alkaline drainage. Consistent with these results, the NP/MPA ratios of samples O (−0.3), WEP (0.1), P1C (0.01), and P1D (0.65) indicate the formation of an acidic effluent. Acidic surface (AMD-1) and groundwater (GW-1,3) samples collected from near the ore (O) and ore-rich wastes (P1C, WEP) agreed well with the NP/MPA ratios. The good consistency between NP/MPA ratios, short and long term paste pH, suggest that

Table 3 Summary of ABA and NAG test results

Sample	Paste pH	Paste EC (µS/cm)	Long-term Paste pH	Long-term Paste EC	Fizz rating	S (%)	APP (kg H_2SO_4/t)	NP (kg $CaCO_3$/t)	NNP (kg $CaCO_3$/t)	ANC (kg H_2SO_4/t)	MPA	NAPP	NPR	NAG_{pH}	NAG (kg H_2SO_4/t)
Wastes															
O[a]	3.2	6620	2.6	n.d	Slight	18.9	591	−217.5	−808.5	−213.15	578.34	791.49	−0.4	2.4	206.5
OBR-1	7.6	1501	n.d	n.d	Slight	1.08	34	37.5	3.8	36.75	33.05	−3.702	1.1	2.5	100.0
OBR-2	7.9	515	7.2	n.d	Moderate	0.17	5.2	275	269.8	269.5	5.205	−264.30	52.6	6.5	1.4
OBR-3	8.1	440	7.6	n.d	Moderate	0.08	2.6	287.5	284.9	281.75	2.45	−279.30	111.4	7.1	*
WEP[b]	3.9	9650	2.6	n.d	Slight	15.46	483	47.5	−435.6	46.55	473.08	426.53	0.1	2.4	147.0
P1C	3.0	6770	2.9	9200	No	15.88	496	−6.5	−502.6	−6.37	485.93	492.29	−0.01	2.1	111.7
P1D	4.4	1294	4.3	1864	No	0.14	4.3	2.8	−1.6	2.744	4.28	1.54	0.6	5.6	1.2
P10A	7.5	622	7.2	1382	Moderate	0.76	23.7	393.8	370.0	385.924	23.26	−362.67	16.6	2.8	20.8
P10B	7.6	807	7.3	1375	Strong	1.07	33.5	720	686.50	705.6	32.74	−672.86	21.5	7.5	*
Gossan[a]	7.6	257	7.7	343	No	0.25	7.9	−6.0	−14.0	−5.88	7.65	13.53	−0,8	5.1	3.7
Lithological units															
B	8.2	228	n.d	n.d	No	0.06	1.8	37.8	36.0	37.044	1.84	−35.21	21.1	6.5	7.1
R1	7.6	159	7.4	488	No	0.02	0.6	2.0	1.4	1.96	0.61	−1.35	3.2	5.4	4.5
R2	7.7	596	7.5	955	Slight	0.29	9.0	−5.0	−14.0	−4.9	8.87	13.78	−0.6	2.6	5.7
R3	7.7	703	7.6	1076	Slight	0.31	9.6	41.8	32.2	40.964	9.49	−31.48	4.4	4.2	3.7
R4	8.4	135	8.1	191	Moderate	0.02	0.7	362.5	361.8	355.25	0.61	−354.64	517.80	6.7	1.0
R5	8.3	94	8.1	112	Strong	0.01	0.3	73.8	73.50	72.324	0.31	−72.02	246.00	6.7	3.9
R9	7.9	199	7.9	267	Strong	0.04	1.4	*	*	*	1.22	*	*	7.5	*
R10	8.1	94	7.9	209	Moderate	0.02	0.7	342.5	341.8	335.65	0.61	−335.04	489.20	5.5	8.6
P1A	5.6	2620	6.5	3430	Slight	0.29	8.9	2.5	−6.4	2.45	8.87	6.43	0.3	5.4	4.1
P1B	6.4	664	6.9	815	Slight	0.25	7.9	39.0	31.1	38.22	7.65	−30.57	5.0	7.0	*
P1E	7.3	598	7.0	857	Strong	0.24	6.7	792.5	785.80	776.65	7.34	−769.30	117.5	6.8	0.4
P10C	8.1	108	7.7	148	Strong	0.07	2.2	*	*	*	2.14	*	*	6.7	3.9
i51	8.0	182	7.8	401	Strong	0.08	2.5	708.8	706.3	694.624	2.45	−692.17	283.50	5.8	5.5
i52	7.4	151	7.8	358	Slight	0.03	1.0	8.3	7.3	8.134	0.92	−7.22	8.4	5.0	7.6

[a]Average values of six samples

[b]Average values of three samples

Table 4 Guidelines of various screening criteria for ABA and NAG tests

References	Screening criterion				
	NPR	NNP	NAG	Paste pH	Long term Paste pH
1. Price et al. (1997)	<1, Likely AMD potential			pH <4, Acid	
	1–2, Possibly AMD potential			pH >7, Neutral	
	2–4, Low AMD potential				
	>4, None				
2. Soregaroli and Lawrence (1998)	<1, PAF				
	1–3, Inconclusive				
	>4, Has enough neutralizing capasity				
3. Brodie et al. (1991)	<1, Acid generating				
	1–3, Uncertain				
	>3, None acid generating				
4. Ferguson and Morin (1991)		<−20, PAF			
		−20 < NNP < 20 Uncertain			
		>20, NAF			
5. Sobek et al. (1978)		<−5, Acid forming			
6. Day (1989)		<10, Acid forming			
7. Sahoo et al. (2014)			NAG <50, NAGpH >5, Non-acid generating		
			NAG <50, NAGpH <5, Moderate acid generating		
			NAG >50, NAGpH <5, High acid generating		
8. Smart et al. (2002)			NAPP <0, NAGpH >4.5, NAF		
			NAPP >0, NAGpH <4.5, PAF		
			NAPP <0, NAGpH <4.5;UC if positive		
			NAPP >0, NAGpH >4.5 UC if negative		
9. This study					pH <4, Acid
					pH >7, Neutral

the NP/MPA ratio of a sample can be a better indicator for predicting post-mining water quality.

Despite the consistency among all the tests methods, several limitations and errors related to the methods have been observed (Abrosimova et al. 2015; Blodau 2006; Dold 2017). These discrepancies were generally attributed to the sulfur mineralogy of the wastes and proton liberation mechanisms (e.g. Fe(III) oxyhydroxides) during dissolution and oxidizing reactions (Dold 2017; Blodau 2006). Consistent with the previous studies, the influence of mineralogy on acid production and consumption reactions was particularly observable in the OBR-1 samples (Table 3). Nevertheless consistency in results from the ABA and NAG tests in previous studies and this study validates that these tests can be used for preliminary evaluation of AMD generation and its influence on water quality (e.g. surface and groundwater) after and/or during mining.

Sources of AMD and Potential Contamination in the Vicinity of the Küre VSM Deposit

Leaching tests conducted on the waste and lithological units indicate that significant concentrations of contaminants may release into solution from the waste materials

Table 5 Evaluation of consistency among screening criteria applied in different tests and classification of samples

Sample	NPR[1]	NPR[2]	NPR[3]	NNP[4]	NNP[5]	NNP[6]	NAG [7]	NAG[8]	Paste pH[1]	Long term Paste pH[9]
Wastes										
O	Likely	PAF	Acid	PAF	Acid	Acid	HAG	PAF	Acid-generating	Acid-generating
OBR-1	Possibly	Inconclusive	UC	UC	Non-acid	Acid	HAG	UC	Acid-neutralizing	*
OBR-2	Non-acid	Insignificant	Non-acid	NAF	Non-acid	Non-acid	Non-acid	NAF	Acid-neutralizing	Acid-neutralizing
OBR-3	Non-acid	Insignificant	Non-acid	NAF	Non-acid	Non-acid	Non-acid	NAF	Acid-neutralizing	Acid-neutralizing
WEP	Likely	PAF	Acid	PAF	Acid	Acid	HAG	PAF	Acid-generating	Acid-generating
P1C	Likely	PAF	Acid	PAF	Acid	Acid	HAG	PAF	Acid-generating	Acid-generating
P1D	Likely	PAF	Acid	UC	Non-acid	Acid	Non-acid	UC	Acid-generating	Acid-generating
P10A	Non-acid	Neutralizing	Non-acid	NAF	Non-acid	Non-acid	MAG	UC	Acid-neutralizing	Acid-neutralizing
P10B	Non-acid	Neutralizing	Non-acid	NAF	Non-acid	Non-acid	Non-acid	NAF	Acid-neutralizing	Acid-neutralizing
Gossan	Likely	PAF	Acid	UC	Acid	Acid	MAG	UC	Acid-neutralizing	Acid-neutralizing
Lithological units										
B	Non-acid	Insignificant	Non-acid	NAF	Non-acid	Non-acid	Non-acid	NAF	Acid-neutralizing	Acid-neutralizing
R1	Low	Insignificant	Non-acid	UC	Non-acid	Acid	Non-acid	NAF	Acid-neutralizing	Acid-neutralizing
R2	Likely	PAF	Acid	UC	Acid	Acid	MAG	PAF	Acid-neutralizing	Acid-neutralizing
R3	Non-acid	Neutralizing	Non-acid	NAF	Non-acid	Non-acid	MAG	UC	Acid-neutralizing	Acid-neutralizing
R4	Non-acid	Insignificant	Non-acid	NAF	Non-acid	Non-acid	Non-acid	NAF	Acid-neutralizing	Acid-neutralizing
R5	Non-acid	Insignificant	Non-acid	NAF	Non-acid	Non-acid	Non-acid	NAF	Acid-neutralizing	Acid-neutralizing
R9	*	*	*	*	*	*	*	NAF	Acid-neutralizing	Acid-neutralizing
R10	Non-acid	Insignificant	Non-acid	NAF	Non-acid	Non-acid	Non-acid	NAF	Acid-neutralizing	Acid-neutralizing
P1A	Likely	PAF	Acid	UC	Acid	Acid	Non-acid	UC		
P1B	Non-acid	Neutralizing	Non-acid	NAF	Non-acid	Non-acid	Non-acid	NAF	-	-
P1E	Non-acid	Insignificant	Non-acid	NAF	Non-acid	Non-acid	Non-acid	NAF	Acid-neutralizing	Acid-neutralizing
P10C	*	*	*	*	*	*	*	NAF	Acid-neutralizing	Acid-neutralizing
i51	Non-acid	Insignificant	Non-acid	NAF	Non-acid	Non-acid	Non-acid	NAF	Acid-neutralizing	Acid-neutralizing
i52	Non-acid	Insignificant	Non-acid	UC	Non-acid	Acid	NAF	NAF	Acid-neutralizing	Acid-neutralizing

PAF potential acid forming, *UC* uncertain, *NAF* non acid forming, *HAG* high acid generation, *MAG* moderate acid generation

*Not subjected to respective AMD prediction test

characterized as acid producing on various static test methods (Table 3; Fig. 7). The results of the leaching test simulated weathering to predict the composition of the runoff, and were compared with the chemistry of the water samples collected from streams close to the mining operations and from the Bakibaba underground mine tunnels to predict potential AMD generation and potentially toxic leachates. Furthermore, the results of the leaching tests were compared with water-quality guidelines for the protection of aquatic life standards (USA EPA-HQ-OW 2015). The determination of the Cu, Cd, and Zn toxicity levels were based on a hardness of 100 mg/L $CaCO_3$ (USA EPA-HQ-OW 2015).

The pH of the leachate from the ore rich (O), P1C, P1D, and WEP wastes was less than 4.5, which indicates that the wastes will produce an acidic runoff. In fact, water samples (AMD 1–3) collected from the Karanlık stream had typical AMD characteristics (Fig. 1; Table 6). The OBR 1, 2, and 3 samples did not produce acidic water. Leaching test results generally agreed with the ABA test results, except for P1A. The PIA sample did not produce an acidic discharge during the leaching test, whereas a slightly acidic runoff, with a long term paste pH of 6.5 and a paste pH value of 5.6, was measured during ABA tests (Fig. 7; Table 3). The inconsistency between the long-term paste pH obtained from the leaching test and paste pH from ABA tests could be due to the P1A sample's mineralogical composition (silicate and pyrite). It is well documented that silicates and oxides contribute minimal acid neutralization due to their slow dissolution kinetics compared to sulfide oxidation. The rate of pyrite oxidation was likely faster than silicate dissolution during the paste pH test (3 weeks) producing an acidic discharge versus the long term paste pH test (3 months). The paste pH and EC results correlated perfectly with the long-term paste pH and EC values

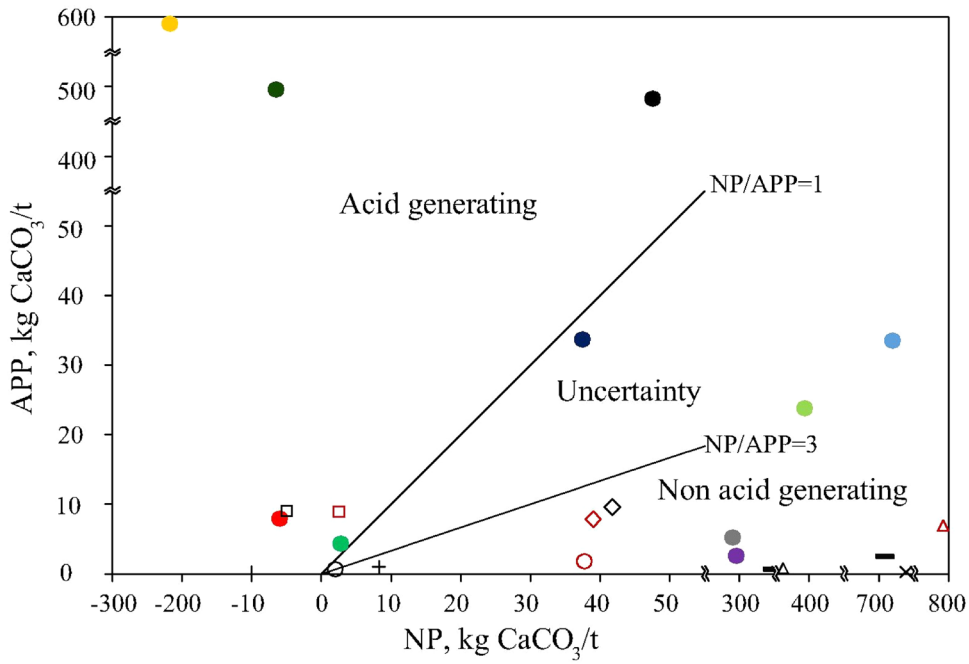

Fig. 4 Evaluation of acid generation potentials using ABA test (Sobek et al. 1978; Brodie et al. 1991; Lapakko 2002)

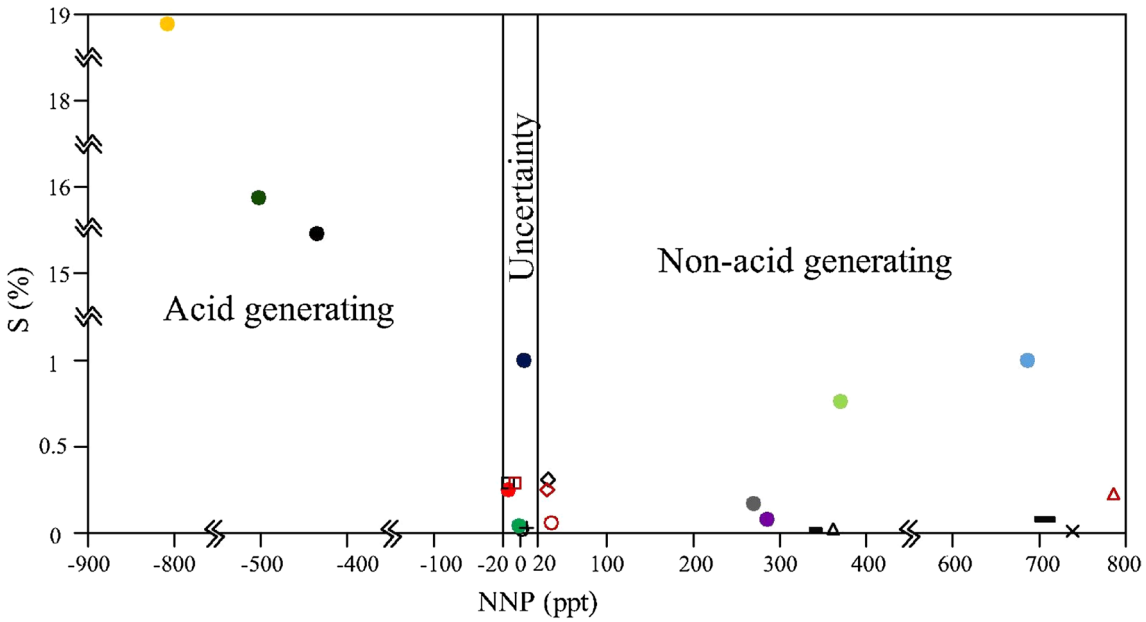

Fig. 5 Evaluation of ABA results using NNP criterion (Ferguson and Morin 1991)

(Table 5). The salinity increased with decreasing pH, indicating dissolution by the acidic solution.

The major anion in all of the leachate solutions was sulfate. Mg, Ca, Si, Na, and K were the dominant cations and the highest Mg and Ca concentrations were generally associated with the acidic samples (Fig. 7). The Cu concentrations in the O, P1C, P1D, and Gossan leachates, which classified as acid producers in the ABA tests, exceeded the USA's acute stream water quality standard (Fig. 7; USA EPA-HQ-OW 2015). The greatest amount of Cu leached from the ore-rich samples (O), which contained the most Cu in the bulk geochemical analysis (44,010 ppm)

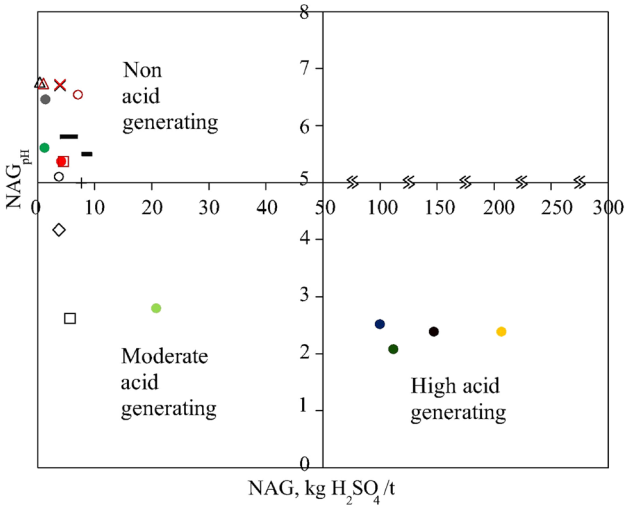

Fig. 6 Evaluation of net acid generation potentials with NAG test (Miller et al. 1997; Sahoo et al. 2014)

and the least from the R1 and R5 samples, which had low acid production rates and Cu content (Fig. 7; Table 1). In general, Cu concentrations in the bulk geochemical analysis correlated with Cu concentrations in the leachate chemistry and APP (Fig. 2).

The Zn concentration in O, PIC, P1D, Gossan, and P1A exceeded the acute aquatic toxicity guideline; R9 and R5 were near the limit (USA EPA-HQ-OW 2015). Leachate from the ore-rich samples (O) contained anomalous Zn levels (9590 ppm) (Fig. 7), but the P1C, P1D, and P1A samples also contained significant amount of Zn. In general, leachates with a high Cu content also contained high amounts of Zn (Fig. 7). An exception was the R9 and R5 samples, which contained a significant amount of Zn in bulk analysis and in the leachate, but low amounts of Cu in both, perhaps due to the pH of leachates (Table 1; Fig. 7).

Samples P10B and P1C exceeded the toxicity guidelines for Pb. It is interesting to note that leachate from ore-rich samples (O) with anomalously Pb content in bulk analysis (385 ppm) did not exceed the toxicity level (Fig. 7). Most likely, some of the Pb precipitated as anglesite (PbSO4) due to the acidic nature of the leachate as suggested by previous studies (Çelik-Balci 2010; Sanlıyuksel et al. 2016).

The Cd concentration in the leachate from O, P1C, P1D, Gossan, and P1A exceeded the toxicity level and was consistent with the bulk analysis. The As concentrations were under the toxicity level (362 ppb) in all leachates; generally, the highest As concentration was associated with the ore-rich wastes. Leachates with high As contents correlated with bulk analysis. The greatest As concentration released from the pyritic copper ore samples was 613 ppm (Tables 1, 2; Fig. 7).

The acidic samples (P1C, P1D, and O) exceeded the toxicity level for Ni (Fig. 7). In general, samples identified as basalt and basalt-basaltic andesite (e.g. P1A and P1B) contained significant amount of Ni (Tables 1, 4). Nevertheless, more Ni leached from the samples with acidic leachates. This was also the case for Co. The most extreme leachate chemistry was obtained from the ore-rich samples (O) and ore-bearing P1C and P1D samples, which contained the highest concentrations of Fe, Cu, Zn, Pb, and As, in addition to Cd, Co, and Ni (Fig. 7).

The leachate composition from the leaching tests were compared with water chemistry data (Fig. 8; Table 6). The drainage system in the district displays diverse characteristics, with pHs ranging from 3.6 to 8 for surface water and 2.9 to 8.3 for groundwater. The AMD was particularly noticeable where the Karanlık stream crosses the ore, ore-rich wastes, and O, P1C, and P1D wastes (Fig. 1). Acidic surface and groundwater samples with low pH and high metal and SO_4^{2-} concentrations plotted around the sample (P1D), which was classified as acid producing by the ABA tests (Tables 3, 4, 5). In contrast to the acidic surface and groundwater, neutral and/or sub-alkaline surface and groundwater samples with low metal concentrations were clustered around the samples classified as non-acid producers, based on the ABA tests (Table 3; Figs. 4, 5). The consistency among paste pH, long term paste pH, and in situ pH measurements of all of the water samples (acidic and neutral surface- and ground-water) suggest that paste pH was a reliable way to quickly assess acid generation and neutralization processes in the region.

Conclusion

Various methods and criteria were used to classify and assess the APP of the waste rock and lithological units around the Küre deposits to identify possible AMD generation sources. The most common sulfur minerals identified in the wastes were pyrite and chalcopyrite. Calcite, dolomite, feldspar, muscovite, quartz, chloride, albite, kaolinite, illite, olivine, and gypsum were common gangue minerals. Waste rock can also be a significant contaminant source (e.g. Cu, Pb, Co, As, Ni, Cd), despite the presence of carbonate minerals.

The maximum AP for the district was associated with the ore-rich wastes, with the highest APP (591), MPA (578.34), NAPP (791.5), and NAG (206.5) values. The P1E sample, with NP (792.5), NNP (785.8), and ANC (694.3) values, represented the maximum value for the district. Considering all of the samples, the NP generally exceeded the APP, indicating that the Küre VSM deposit waste rocks generally have a low AMD potential. Importantly, the long-term paste pH from the leaching tests had

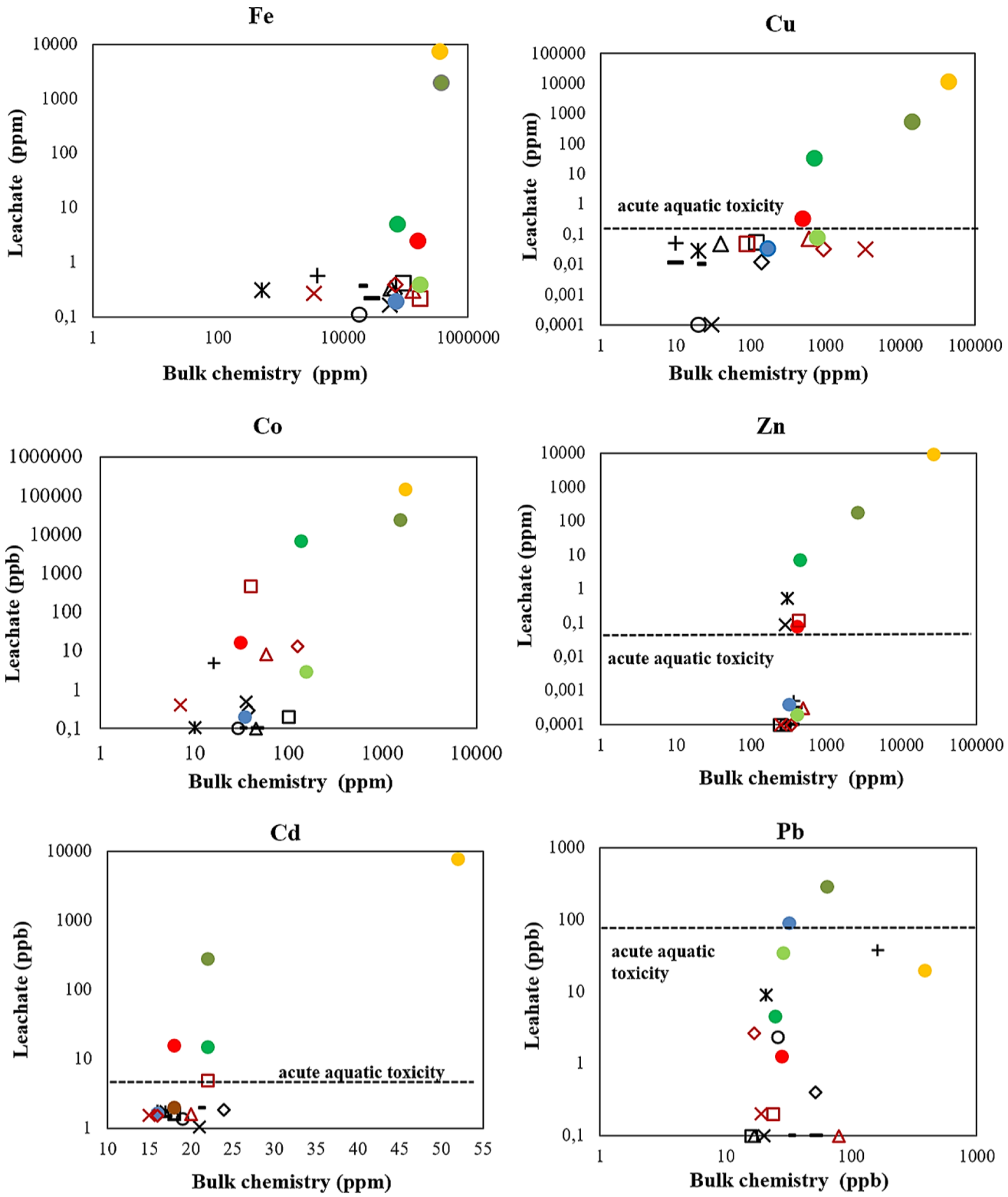

Fig. 7 Bulk geochemical results for metal concentrations versus the concentration of metals in leachate. (Note some of log scale, acute water quality standard—USA-EPA HQ-OW 2015)

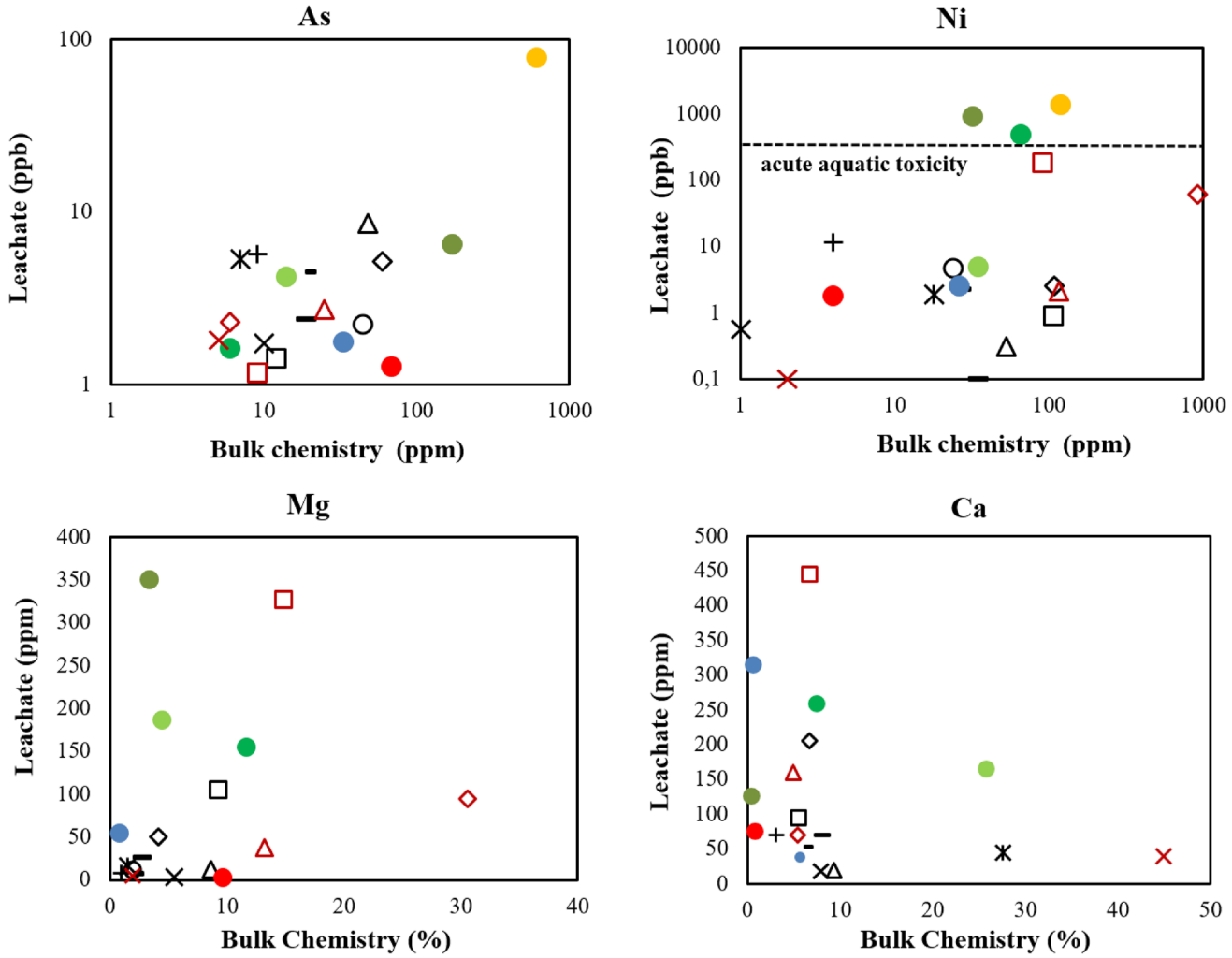

Fig. 7 (continued)

neutral to sub-alkaline pH values and low metal concentrations. The aqueous extracts of some of the samples (O, P1C, P1D, and WEP) were acidic during the leaching tests. Consequently, acid drainage could occur over long periods of interaction between the waste rocks and water. During oxidation of the waste rocks (O, P1C, P1D), contaminants in the leachate solution often exceeded the acute aquatic toxicity level. Low pH and increasing concentrations of sulfate and contaminants (e.g. Cu, Zn, Co, Cd, Pb, As) suggest that sulfide mineral oxidation mainly occurs in the O, P1C, and P1D waste rock. From the ABA and NAG tests, it appears that the NP of the district was generally higher than the APP of the wastes. Field water quality data correlated well with ABA and long term paste pH tests, indicating the acidic drainage associated with the O, P1C, and P1D wastes. Furthermore, NP/MPA ratios were found to be a better indicator of post-mining drainage quality. Consistent results between NPR, NP, APP, MPA, NP and long-term leachate chemistry along with field water quality data affirmed that static tests can be used for preliminary evaluation of possible AMD generation. However, site-specific geochemical and mineralogical conditions should be well defined and results of the ABA and NAG tests should be combined for proper environmental assessments. ABA tests, geochemical, mineralogical, and leaching studies of the Küre wastes and lithological rocks indicated that the likelihood of AMD formation was curbed by the high NPs of the ultramafic rocks. The storage of wastes (O) with the highest APP value around the sample with the highest NP value (PIE) is suggested to prevent local AMD generation near the Karanlık stream.

Table 6 Selected water chemistry data of Küre groundwater and surface water drainage system

Sample	pH	EC (µS/cm)	SO_4^{2-} (mg/l)	Fe (ppm)	Cu (ppm)	Zn (ppm)	Co (ppm)	Ni (ppm)	Mn (ppm)	Cr (ppm)	Pb (ppm)	Cd (ppm)	As (ppm)
Acidic surface water													
AMD-1	3.6	3430	2150	16.7	68	43.2	10.1	5	42.4	0.06	0.02	0.04	0.005
AMD-2	4.1	2660	2450	11.7	55.2	33.2	8.9	1.2	35.1	0.03	0.01	0.03	0.004
AMD-3	4.2	2740	1600	14.3	32.1	25.3	4.7	0.5	22.7	0.01	0.01	0.02	0.001
Average (n = 3)	4.0	2943.3	2066.7	14.2	51.8	33.9	7.9	2.2	33.4	0.0	0.01	0.03	0.00
Neutral surface water													
SW	8.1	0.5	0.7	0.2	0.4	0.2	0.02	0.01	0.09	0	0.01	0.01	0.001
SW	8.2	0.3	0.7	0.02	0.14	0.2	0.02	0.01	0.07	1	0.001	0.01	0.001
Acidic groundwater													
GW-1 (780 m)*	2.9	2.9	1050	19.6	0.1	9.9	2.0	0.1	15.5	0.003	0.008	0.01	0.003
GW-3 (690 m)*	4.5	2.3	700	12.4	0.01	0.7	0.9	0.05	8.2	0.002	0.002	0.01	0.001
Average (n = 2)	3.7	2.6	875	16.0	0.07	5.3	1.4	0.08	11.8	0.003	0.005	0.01	0.002
Neutral groundwater													
GW-2 (725 m)*	7.1	2.7	1250	0.2	0.002	0.05	0.3	0.01	5.2	0.001	0.002	0.01	0.001
GW-4 (630 m)*	7.9	0.9	400	0.3	0.007	0.02	0.003		0.2	0.002	0.003	0.01	0.005
GW-5 (512 m)*	8.3	0.3	300	0.03	0.002	0.02	0.0001		0.004	0.003	0.001	0.01	0.007
Average (n = 3)	7.8	1.3	650	0.2	0.004	0.03	0.1	0.01	1.8	0.002	0.002	0.01	0.004
AALC (ppb)					65	120		120			65	<2	

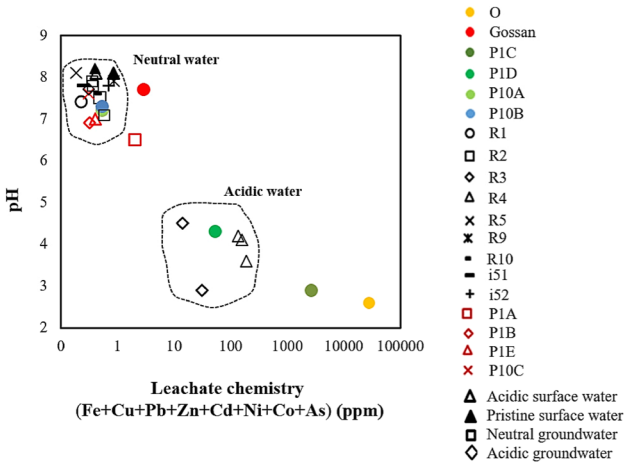

Fig. 8 Correlation of field water quality versus leachate chemistry and pH

Acknowledgements This project was supported by the Istanbul Technical University Scientific Research Division Grant to NB (37260). We thank Dr. Paul Schroeder for his valuable comments on the XRD data and Dr. Aral Okay for kindly providing sandstone samples from the Çağlayan formation (i51, i52; Okay et al. 2014, 2015).

References

Abrosimova N, Gaskova O, Loshkareva A, Edelev A, Bortnikova S (2015) Assessment of the acid mine drainage potential of waste rocks at the Ak-Sug porphyry Cu–Mo deposit. J Geochem Explor 157:1–14

Akabzaa TM, Armah, TEK, Baneong-Yakubo BK (2007) Prediction of acid mine drainage generation potential in selected mines in the Ashanti Metallogenic Belt using static geochemical methods. Environ Geol 52:957–964

Akbulut M, Oyman T, Çiçek M, Selby D, Özgenç İ, Tokçaer M (2016) Petrography, mineral chemistry, fluid inclusion microthermometry and Re–Os geochronology of the Küre volcanogenic massive sulfide deposit (Central Pontides, Northern Turkey). Ore Geol Rev 76:1–18

Altun Y, Yılmazi H, Şiner İ, Yazar F (2015) The secrets of massive sulfide deposits on mid-ocean ridges and Küre Mağaradoruk copper deposit. MTA Bull Min Res Exp 150:51–65 **(in Turkish)**

Bailey EH, Barnes JW, Kupfer DH (1966) Geology and ore deposit of Küre district, Kastamonu province. CENTO summer training program in geological mapping techniques, Turkey, pp 17–73

Balci N, Wayne CS, Mayer B, Mandernack K (2007) Oxygen and sulfur isotope systematics of sulfate by bacterial and abiotic oxidation of pyrite. Geochim Cosmochim Acta 71(15):3796–3811

Balci N, Mayer B, Wayne CS, Mandernack K (2012) Oxygen and sulfur isotope systematics of sulfate produced during abiotic and bacterial oxidation of sphalerite and elemental sulfur. Geochim Cosmochim Acta 77:335–351

Blodau C (2006) A review of acidity generation and consumption in acidic coal mine lakes and their watersheds. Science Total Environ 369:307–332

Bouzahzah H, Benzaazoua M, Bussière B (2013) Acid-generating potential calculation using mineralogical static test: modification of the Paktunc equation. In: Proceedings of 23rd World Mining Congress, Montreal, QC, Canada

Bouzahzah H, Benzaazoua M, Bussière B, Plante B (2014) Prediction of acid mine drainage: importance of mineralogy and test protocols for static and kinetic tests. Mine Water Environ 33:54–65

Boztuğ D, Debon F, Le Fort P, Yılmaz O (1985) Geochemical characteristics of some plutons from the Kastamonu granitoid belt (northern Anatolia, Turkey). Schweiz Miner Petrog 64(3):389–403

Brady KBC, Perry EF, Beam RL, Bisko DC, Gardner MD, Tarantino JM (1994) Evaluation of acid-base accounting to predict the quality of drainage at surface coal mines in Pennsylvania, U.S.A. In: International land reclamation and mine drainage conference and 3rd international conference on the abatement of acidic drainage, 24–29 April 1994, vol 1. SP 06A-94, U.S. Bureau of Mines, Pittsburgh, PA, pp 138–147

Brodie MJ, Broughton LM, Robertson A (1991) A conceptual rock classification system for waste management and a laboratory method for ARD prediction from rock piles. Proc 2nd ICARD 3:119–135

Çakır Ü (1995) Aşıköy-Toykondu (Küre-Kastamonu) massif sülfid yataklarının jeolojik özellikleri. MTA Bull Min Res Exp 117:29–40 **(in Turkish)**

Celik-Balcı N (2010) Effect of bacterial activity on trace metals release from oxidation of sphalerite at low pH (< 3) and implications for AMD environment. Environ Earth Sci 60(3):485–493

Dold D (2017) Acid rock drainage prediction: a critical review. J Geochem Explor 172:120–132

Duncan DW, Bruyensteyn A (1979) Determination of the acid production potential of waste materials. In: Metallurgical Society of AIME Annual Meeting, New Orleans, pp A79–29

Ferguson KD, Morin KA (1991) The prediction of acid rock drainage—lessons from the database. Proc 2nd ICARD 3:85–106

Güner M (1980) Geology and massive sulfide ores of the Küre area, the Pontic ranges, northern Turkey. MTA Bull Min Res Exp 93/94:65–109 **(in Turkish)**

Hageman PL, Seal RR, Diehl SF, Piatak NM, Lowers HA (2015) Evaluation of selected static methods used to estimate element mobility, acid-generating and acid-neutralizing potentials associated with geologically diverse mining wastes. Appl Geochem 57:125–139

Jambor JL (2003) Mine-waste mineralogy and mineralogical perspectives of acid–base accounting. In: Jambor JL, Blowes DW, Ritchie AIM (eds) Environmental aspects of mine wastes, vol 31. Mineralogical Association of Canada, Short course, pp 117–146

Jambor JL, Dutrizac JE, Raudsepp M (2007) Measured and computed neutralization potentials from static tests of diverse rock types. Environ Geol 52:1019–1031

Kuşçu İ, Erler A (2002) Pyrite deformation textures in the deposits of Küre mining district (Kastamonu-Turkey). Turk J Earth Sci 11:205–215

Kwong YTJ (1993) Mine site acid rock drainage assessment and prevention; a new challenge for a mining geologist. In: Proceedings of the international mining geology conference, Kalgoorlie, pp 213–217

Lapakko KA (2002) Metal mine rock and waste characterization tools: an overview, mining, minerals and sustainable development. Report 67, Acid Drainage Technology Initiative, http://pubs.iied.org/pdfs/G00559.pdf

Lawrence RW, Scheske M (1997) A method to calculate the neutralization potential of mining wastes. Environ Geol 32(2):100–106

Lawrence RW, Poling GP, Marchant PB (1989) Investigation of predictive techniques for acid mine drainage. Report on DSS Contract No. 23440-7-9178/01-SQ, Energy Mines and Resources, MEND Report 1.16.1(a), Canada

Lottermoser BG (2010) Mine wastes: characterization, treatment and environmental impacts, 3rd edn. Springer, Berlin, Heidelberg

Miller S, Robertson A, Donahue T (1997) Advances in acid drainage prediction using the net acid generation (NAG) test. In: Proc. 4th international conference on acid rock drainage, Vancouver, BC, pp 533–549

Modabberi S, Alizadegan A, Mirnejad H, Esmaeilzadeh E (2013) Prediction of AMD generation potential in mining waste piles, in the sarcheshmeh porphyry copper deposit, Iran. Environ Monit Assess 185:9077–9087

Mohammadi Z, Modabberi S, Jafari MR, Ajayebi KS (2015) Comparison of different static methods for assessment of AMD generation potential in mining waste dumps in the Muteh Gold Mines, Iran. Environ Monit Assess 187:374

Nordstrom DK, Alpers CN, Ptacek CJ, Blowes DW (2000) Negative pH and extremely acidic mine waters from Iron Mountain, California. Environ Sci Technol 34:254–258

Okay AI, Tüysüz O, Satır M, Özkan-Altıner M, Altıner D, Sherlock S, Eren RH (2006) Cretaceous and Triassic subduction-accretion, HP/LT metamorphism and continental growth in the Central Pontides, Turkey. Geol Soc Am Bull 118:1247–1269

Okay AI, Sunal G, Tüysüz O, Sherlock S, Keskin M, Kylander-Clark ARC (2014) Low-pressure-high temperature metamorphism during extension in a Jurassic magmatic arc, Central Pontides, Turkey. J Metamorph Geol 32:49–69

Okay AI, Altıner D, Kılıç AM (2015) Triassic limestone, turbidite and serpentinite—the cimmeride orogeny in the central pontides. Geol Mag 152(3):460–479

Page AL, Miller RH, Keeney DR (1982) Methods of soil analysis, Part 2, chemical and microbiological properties, Agronomy 9, 2 edn. ASA, Madison

Perry (1998) Interpretation of acid-base accounting. Coal Mine Drainage Prediction and Pollution Prevention in Pennsylvania, PA Dept of Environmental Protection, Harrisburg, pp 11-1–11-18

Plumlee GS (1999) The environmental geology of mineral deposits. In: Plumlee GS, MJ Logsdon (eds) The environmental geochemistry of mineral deposits, Part A. Processes, techniques, and health issues. Reviews in economic geology, vol 6A. Society of Economic Geologists, Littleton, CO, pp 71–116

Price WA, Errington J, Koyanagi V (1997) Guidelines for the prediction of acid rock drainage and metal leaching for mines in British Columbia: part I. General procedures and information requirements. In: Proc, 4th ICARD, Natural Resources Canada, Ottawa, vol 1, pp 1–14

Sahoo PK, Tripathy S, Panigrahi MK, Equeenuddin Sk-Md (2014) Geochemical characterization of coal and waste rocks from a high sulfur bearing coalfield, India: implication for acid and metal generation. J Geochem Explor 145:135–147

Sanliyuksel D, Balci N, Baba A, Alper (2016) Generation of acid mine lakes associated with abandoned coal mines in northwest Turkey. Arch Environ Contam Toxicol 70:757–782

Schippers A (2004) Biogeochemistry of metal sulfide oxidation in mining environments, sediments and soils. In: Amend JP, Edwards KJ, Lyons TW (eds) Sulfur biogeochemistry—past and present, vol 379. Geological Society of America, Boulder, pp 49–62

Shu WS, Ye ZH, Lan CY, Zhang ZQ, Wong MH (2001) Acidification of lead/zinc mine tailings and its effect on heavy metal mobility. Environ Int 26:389–394

Skousen J, Simmons J, McDonald LM, Ziemkiewicz P (2002) Acid–base accounting to predict post-mining drainage quality on surface mines. J Environ Qual 31:2034–2044

Smart R, Skinner WM, Levay G, Gerson AR, Thomas JE, Sobieraj H, Schumann R, Weisener CG, Weber PA, Miller SD, Stewart WA (2002) ARD test handbook: project P387A prediction and kinetic control of acid mine draiange: AMIRA. International Ltd, Ian Wark Research Institute

Sobek AA, Schuller WA, Freeman JR, Smith RM (1978) Field and laboratory methods applicable to overburdens and mine soils. Rept EPA-600/z-78-054, US Environmental Protection Agency, Cincinnati

Soregaroli BA, Lawrence RW (1998) Update on waste characterisation studies. In: Proc. mine design, operations and closure conference, Polson, MT, USA

USA, EPA (US Environmental Protection Agency) (2015) (http://fdsys.gpo.gov/fdsys/search/home.action) and on Regulations.gov (http://www.regulations.gov) in Docket No. EPA-HQ-OW-2016-0012

Ustaömer T, Robertson AHF (1994) Late Paleozoic marginal basin and subduction-accretion: the Paleotethyan Küre Complex, Central Pontides, northern Turkey. J Geol Soc London 151:291–305

Weber PA, Stewart WA, Skinner WM, Weisener CG, Thomas JE, Smart RSC (2004) Geochemical effects of oxidation products and framboidal pyrite oxidation in acid mine drainage prediction techniques. Appl Geochem 19:1953–1974

Wedepohl KN (1995) The composition of the continental crust. Geochim Cosmochim Acta 59(7):1217–1232

Weisener CG, Weber PA (2010) Preferential oxidation of pyrite as a function of morphology and relict texture. N Z J Geol Geophys 53(2–3):167–176